International Journal of Engineering Trends and Technology
ISSN: 2231–5381 / https://doi.org/10.14445/22315381/IJETT-V72I1P118

Volume 72 Issue 1, 184-192, January 2024

Original Article

Performance Improvement of UPQC with Sliding Mode Fractional Order Proportional Integral Control with Enhancement of Harmonics Mitigation

M. Serabanda[1], B. Suresh Kumar[2], G. Mallesham[3]

[1,3]*Department of Electrical Engineering, University College of Engineering, Osmania University, Hyderabad, India.*
[2]*Department of Electrical and Electronics, C.B.I.T, Osmania University, Hyderabad, India.*

Corresponding Author : sharathm84@gmail.com

Received: 30 September 2023 Revised: 20 December 2023 Accepted: 23 December 2023 Published: 07 January 2024

Abstract *- For the increasing load demand in the distribution network there is a vast incline of power quality issues in the system. Due to modern load demand, more nonlinear devices are connected to the network, inducing more harmonics and voltage fluctuations. To mitigate these issues, a UPQC device is recommended to be connected on the load side. The UPQC device comprises series and shunt converters for the reduction of voltage fluctuations and harmonics, respectively. The series controller of UPQC is less complex, with only voltage differentiation calculations, whereas the shunt controller has a voltage regulator. The voltage regulator (PI) is updated by FOPI and SM-FOPI controllers improving the performance of the voltage regulator. A comparative analysis is carried out with different controllers for the shunt converter of UPQC, and the parametric comparisons determine better control modules. All the results and graphs are validated and plotted using MATLAB software.*

Keywords *- UQPC (Unified Power Quality Conditioner), PI (Proportional Integral), FOPI (Fractional order PI), SM-FOPI (Sliding Mode – FOPI), MATLAB (Matrix Laboratory).*

1. Introduction

In modern power systems, there is a gradual increase in electrical power demand as the number of loads and previous load capacities are increasing. Most urban networks need electrical power for production and manufacturing goods for utility. In the present scenario, new nonlinear loads are in great increments, demanding more power from the grid. These nonlinear loads are electric vehicle (EV) charging stations that use high-rated power electronic devices for the conversion of voltages [1]. The EV batteries need very high power for charging, leading to the injection of huge harmonics in the network, which may impact other regular loads [2]. To avoid these harmonics entering the network and reduce the effect on the regular loads, an Active Power Filter (APF) device needs to be connected at the charging station.

The APF connected at the load side filters the harmonics generated by the nonlinear charging station.Previous research has shown that Flexible AC Transmission (FACT) devices are used to compensate for harmonics and stabilize voltage. To stabilize voltage, a Dynamic Voltage Restorer (DVR) is connected in series to the line. These devices are connected at the load and source side and are operated with individual controllers. However, this can cause unsynchronized operation and require an extra DC source for the DVR device, which increases the cost of the modules. To address this issue, a combined FACT device, which can perform both voltage stabilization and harmonic compensation with a single device, is recommended.

This device can be UPQC, which is integrated with a 6-IGBT switches series converter and a 6-IGBT switches shunt converter connected back-to-back with a DC link capacitor connected. The series converter mitigates the voltage fluctuations caused on the network side through series transformers connected to the lines [4]. The shunt converter mitigates or filters the harmonics caused by the nonlinear load (EV charging station) by connection in parallel to the load. These two converters are connected on the DC to a common capacitor for storage and injection of power into the system. Each converter is integrated with filters for conversion of PWM AC voltages to Sin voltages [5]. The series transformers connected have a specific turn ratio with respect to DC link voltage. The complete configuration of the test system network with nonlinear load can be seen in Figure 1.

As defined in Figure 1, the source voltages and currents are denoted as V_{sabc} and I_{sabc}, Load voltages and currents are given as V_{Labc} and I_{Labc}, Series filters are R_{sr}, L_{sr} and C_{sr}, Shunt filters are R_{sh}, L_{sh} and C_{sh}, series injected voltages are V_{srabc}, shunt compensation currents are I_{srabc}. The series converter has 6-IGBT switches (S1-S6) and shunt converter has 6-IGBT switches (P1-P6) [6]. These switches are controlled by individual control modules operated by different PWM techniques for voltage and harmonics compensation. The series converter is controlled by the Sin PWM technique, and the shunt converter is controlled by the hysteresis current controller [7].

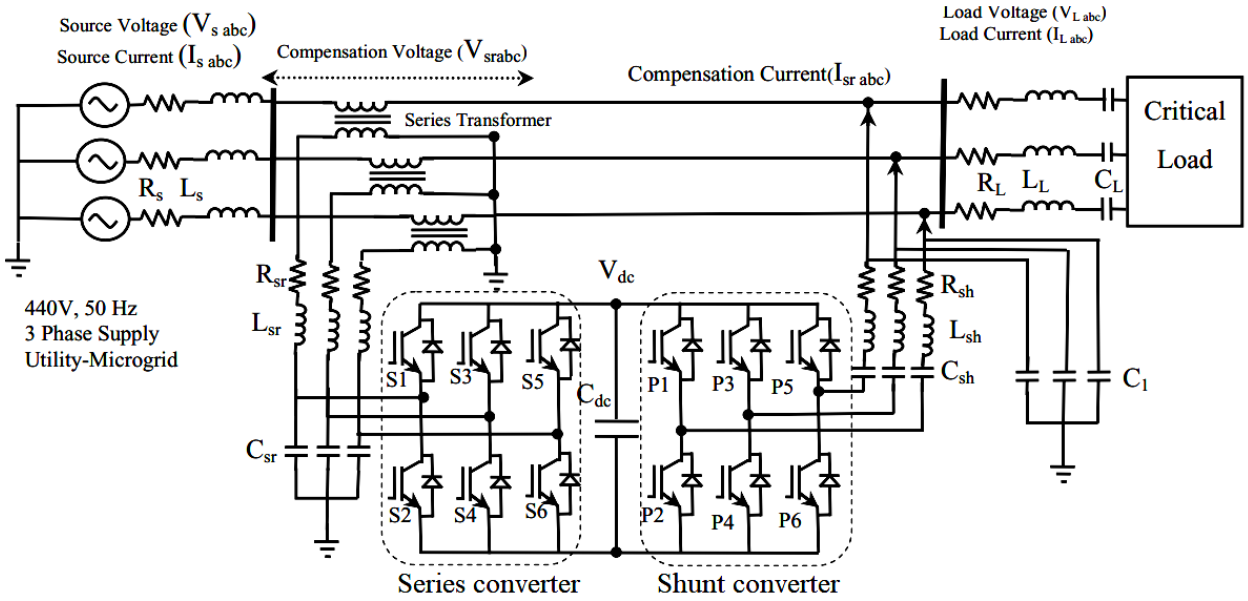

Fig. 1 UPQC configuration with nonlinear critical load

The purpose of this study is to compare different controllers integrated into the shunt voltage controller to improve the performance of the UPQC device. The controllers that were considered are the conventional PI controller, FO-PI controller, and SM-FO-PI controller. The conventional PI controller is a traditional module with fixed Kp and Ki values, which has higher disturbances and oscillations with lower harmonic mitigation. The FO-PI controller is a fractional order integral gain controller which has better performance than the conventional PI controller. FO-PI has lesser damping, which increases harmonics mitigation further. Lastly, the SM-FO-PI controller is a three-variable sliding controller that varies the Kp, Ki, and fractional order gains. This controller has very little damping and has a faster response rate, which reflects on the maximum reduction of harmonic content in the system.The paper is organized with section I introducing the proposed UPQC topology and the network diagram for testing the circuit module. The design and configuration of UPQC and its controller modules are given in section II. In section III, the modeling of proposed control structures FOPI and SM-FOPI are discussed. The simulation of these proposed systems by different controllers is carried out in MATLAB Simulink software, with a comparative analysis presented in section IV.

The final section, V, has a conclusion to this paper validating the results and finalizing the optimal controller, followed by references in the paper.

2. Design of UPQC

As mentioned previously, the UPQC comprises two 6-IGBT switch converters, which are connected in series and shunt to the grid [8]. Each bridge is operated by individual control modules taking feedback from the source side and load side. The series converter is controlled with feedback from V_{sabc} and V_{Labc} with synchronization using PLL (Phase Locked Loop). The shunt converter is controlled with feedback from I_{Labc}, V_{sabc} and I_{srabc}[9]. Both converters operate in synchronization with the source voltages V_{sabc}, avoiding harmonic generation in the system.

2.1. Series Converter Control

The series converter control is a voltage-based control scheme where the difference of deficit voltage is determined for compensation. Voltage is injected into the grid through individual connected series transformers to each phase as the injected voltages may be unbalanced [10]. The series transformers are connected to a series converter through an LC filter for harmonics reduction. The series control structure is designed as in Figure 2.

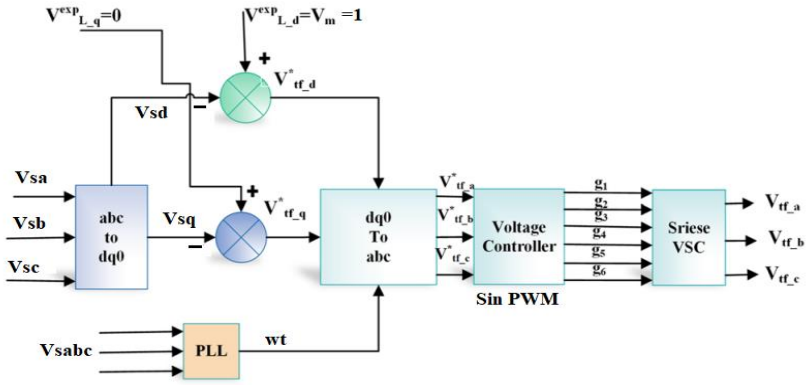

Fig. 2 Series converter structure

Initially, the source voltages are converted to dq components using the park's transformation given as

$$\begin{bmatrix} V_{sd} \\ V_{sq} \\ V_{s0} \end{bmatrix} = \begin{bmatrix} Sin\ wt & -Cos\ wt & 0 \\ Cos\ wt & Sin\ wt & 0 \\ 0 & 0 & 1 \end{bmatrix} \begin{bmatrix} V_{sa} \\ V_{sb} \\ V_{sc} \end{bmatrix} \quad (1)$$

These measured source voltage dq components (VsdVsq) are compared to reference dq components $V_{L\_d}^{exp}$ *and* $V_{L\_q}^{exp}$ taken as 1 and 0, respectively [11].

$$V_{tf\_d}^{*} = V_{L\_d}^{exp} - V_{sd} \quad (2)$$

$$V_{tf\_q}^{*} = V_{L\_q}^{exp} - V_{sq} \quad (3)$$

The difference of the dq components is converted back to abc using inverse park's transformation given as

$$\begin{bmatrix} V_{tf\_a}^{*} \\ V_{tf\_b}^{*} \\ V_{tf\_c}^{*} \end{bmatrix} = \begin{bmatrix} Sin\ wt & Cos\ wt & 1 \\ Sin\left(wt - \frac{2\pi}{3}\right) & Cos\left(wt - \frac{2\pi}{3}\right) & 1 \\ Sin\left(wt + \frac{2\pi}{3}\right) & Cos\left(wt + \frac{2\pi}{3}\right) & 1 \end{bmatrix} \begin{bmatrix} V_{tf\_d}^{*} \\ V_{tf\_q}^{*} \\ V_{tf\_0}^{*} \end{bmatrix} \quad (4)$$

These reference signals $V_{tf\_a}^{*}, V_{tf\_b}^{*}, V_{tf\_c}^{*}$ are compared to high frequency triangular waveforms generating signals for S1-S6 switches of series converter as in Figure 3. The series voltage $V_{tf\_a}, V_{tf\_b}, V_{tf\_c}$ from the series, converters are injected into the line through the series transformers with a 1:1 turns ratio compensating for the deficit sag voltages.

2.2. Shunt Converter Control

The shunt converter control is a current-based control scheme where the load currents are considered for the harmonics compensation. For synchronization of the shunt converter currents to the grid source, voltages are considered for PLL [12]. The shunt converter control design can be observed in Figure 4. Along with I_{Labc} and V_{sabc}, the DC link voltage V_{dc} across the capacitor, C_{dc} is also measured. The dq components of the load voltages are calculated using equation (1), replacing voltages with currents.

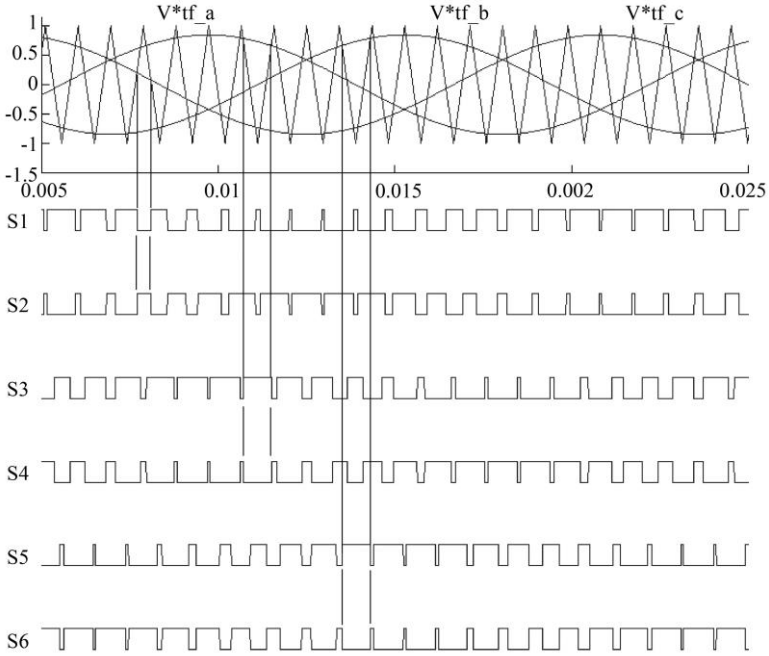

Fig. 3 Sin PWM technique voltage controller

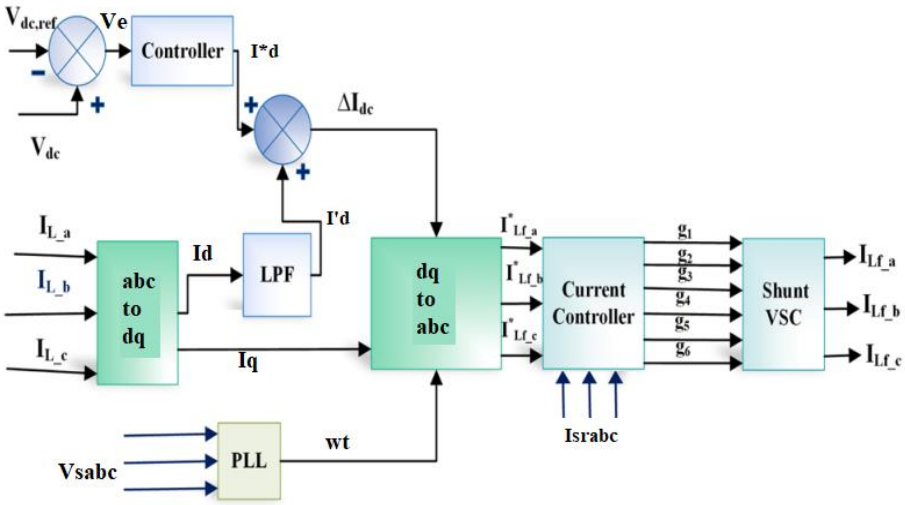

Fig. 4 Shunt converter control design

The generated ID component is filtered by LPF (Low Pass Filter), eliminating disturbances in the signal generating new filtered component I_d' [13].

This filtered component is added to the reference component generated by the DC voltage controller with input from the DC voltage comparison. The DC voltage controller is basically a PI controller with specific K_p and K_i gains generating reference d-axis component given as

$$I_d^* = (V_{dc\,ref} - V_{dc})\,(K_p + \int K_i.dt) \quad (5)$$

The new current d component ΔI_{dc} is given

$$\Delta I_{dc} = I_d^* + I_d' \quad (6)$$

There is no change in the current q component, and it is directly considered for the inverse park's transformation by equation (4) converting ΔI_{dc} and Iq to abc. The reference current signals $I_{Lf\_a}^*$, $I_{Lf\_b}^*$, $I_{Lf\_c}^*$ are the compensating harmonic current signals.

The pulses for the shunt converter switches P1-P6 are generated by the hysteresis current controller comparing $I_{Lf\_a}^*$, $I_{Lf\_b}^*$, $I_{Lf\_c}^*$ signals with shunt converter currents I_{srabc}. The hysteresis current controller generates signals to the shunt converter, as shown in Figure 5.

The hysteresis comparator is defined with the upper hysteresis band (UHB) and lower hysteresis band (LHB) [14]. The comparator is operated as per the error signals generated by the comparison of reference signals, which are measured signals. The shunt converter switches P1-P6 are controller according to the signals generated by the hysteresis comparator.

The compensation currents Israbc are injected into the load sideline, mitigating the current harmonics generated by the nonlinear load. To improve the performance of the shunt converter, the conventional PI controller can be replaced with advanced control modules for further reduction of harmonics in the system. New adaptive controllers, replacing the traditional PI controller, are discussed in the next section.

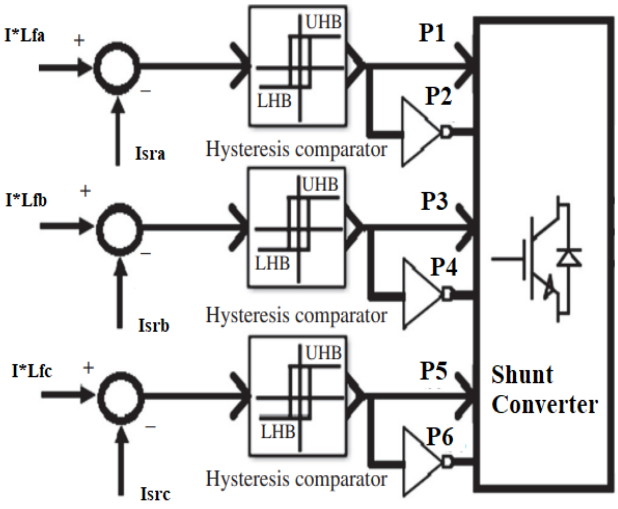

Fig. 5 Hysteresis current controller in shunt control

3. FOPI AND SM-FOPI Control Modules

The fractional order PI controller (FOPI) is an advancement to the PI controller with a reduced order integral operator [15]. The proportional gain (Kp) of the FOPI controller has remained the same, and the integral gain (Ki) order is updated with fractional value. The FOPI reduced order is mathematically represented as

$$g(s) = K_p + \int \frac{K_i}{s^\lambda} \quad (7)$$

In the given equation (7), the fractional order λ ranges between 1 and 0. At lower values of λ, the response of the controller is exponentially increased, and at higher values of λ, the response is reduced. The value of λ is decided by the damping of the DC voltage regulator and the settling of DC link voltage at the reference set value as per the requirement of the network [17]. The controller modelling can be seen in Figure 6.

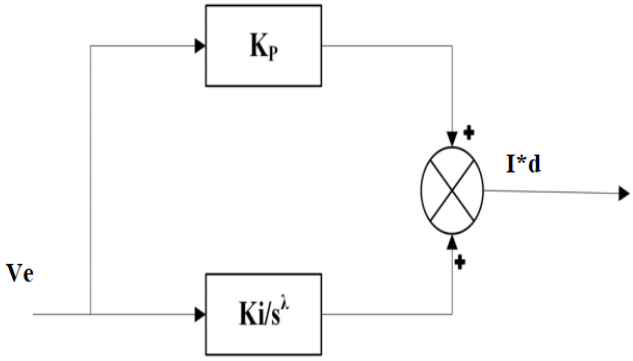

Fig. 6 FOPI controller design

In the given Figure 6, the input is the error voltage generated by DC link voltage (Vdc) comparison with reference voltage (Vref). The output of the control module I*d is updated to load the current d-component. In a further modification of the FOPI control module, the Kp, Ki, and λ values are varied as per the error input with sliding mode control law policy [18] [19]. With the update of sliding gains of the controller, the response of the DC voltage regulator is further improved. This improves the performance of UPQC, and harmonics in voltages and currents are further reduced [20]. The design of the SM-FOPI controller can be observed in Figure 7.

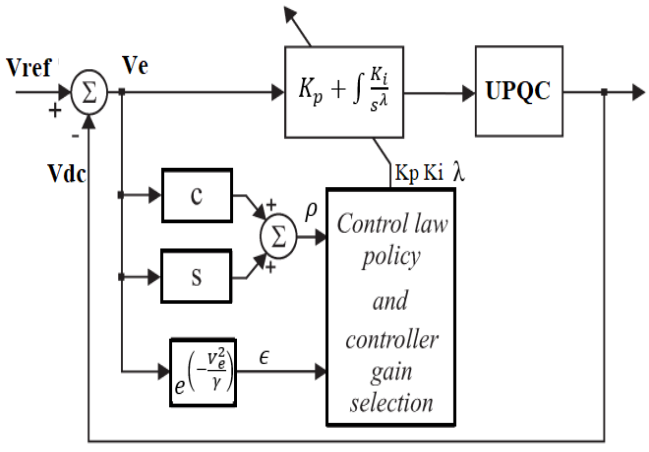

Fig. 7 SM-FOPI control module design

The control law policy and controller gain selection module depend on the values of ρ and ϵ, which are generated by the given equations below [21].

$$\epsilon = e^{\left(-\frac{V_e^2}{\gamma}\right)} \tag{8}$$

$$\rho = Ve(c+s) \tag{9}$$

In the above-given equations (8) and (9), γ is given as 500, c=10 and s=100. From these values, the Kp, Ki and λ are determined as per the below-given expressions.

$$K_p = \left[\left(1 + sign(\rho)K_p^+ - \left(1 - sign(\rho)\right)K_p^-\right] + K_p^{avrg} \tag{10}$$

$$K_i = \left[\left(1 + sign(\rho)K_i^+ - \left(1 - sign(\rho)\right)K_i^-\right] + K_i^{avrg} \tag{11}$$

$$\lambda = \frac{1}{e^{Ve}} \tag{12}$$

As per given equations (10) and (11), the gain values are given in Table 1. The λ value for the integral gain order is inversely proportional to the voltage error (Ve) [22]. For the larger value of Ve, the λ value becomes near zero. When the error voltage is approximately zero, the λ becomes '1', making it a simple integral gain order. The controller response majorly improves during the initial transient and for any disturbances in the system [16]. A comparative analysis is carried out on test systems with different control modules, which include PI, FOPI and SM-FOPI controllers in the next section.

Table 1. SM-FOPI gains

K_p^+=0.01	K_p^-=0.005	K_p^{avrg}=0.1
K_i^+=0.000012	K_i^-=0.00045	K_i^{avrg}=0.00023

4. Results and Analysis

The complete modeling of the system is done in Simulink of MATLAB software with blocks considered from the 'Powersystem' block set. The parameters of the test system network are taken from Table 2.

Table 2. Test network parameters

Name of the parameters	Values
Grid	415V 50Hz Rs=0.1Ω, Ls=0.7mH.
Nonlinear load	Diode bridge rectifier connected R load = 100Ω
UPQC	Cdc=750uF,Rse=1Ω, Cse=100uF, Series T/F – 1:1 turns ratio, 4kVA 50Hz, Lf=10mH
Series controller	d ref = 1; q ref = 0, LPF (F_o)=200Hz
Shunt controller	Vdc ref = 700V, Kp=2, Ki=0.005 Hysteresis band = ±0.01

As per the above-given parameters in Table 2, the simulation is updated and run for 1sec, and the results are generated for all the voltages and powers of the system. The graphs of the measured signals are plotted with respect to time. Voltage sag and swell are created in the system using a programmable voltage source varying the amplitudes of the voltages at different time intervals. Voltage sag of 0.7pu is created from 0.2-0.4sec, and voltage swell of 1.3pu is created from 0.6-0.8sec. The harmonics in the source current and load voltages, however, are created by nonlinear load.

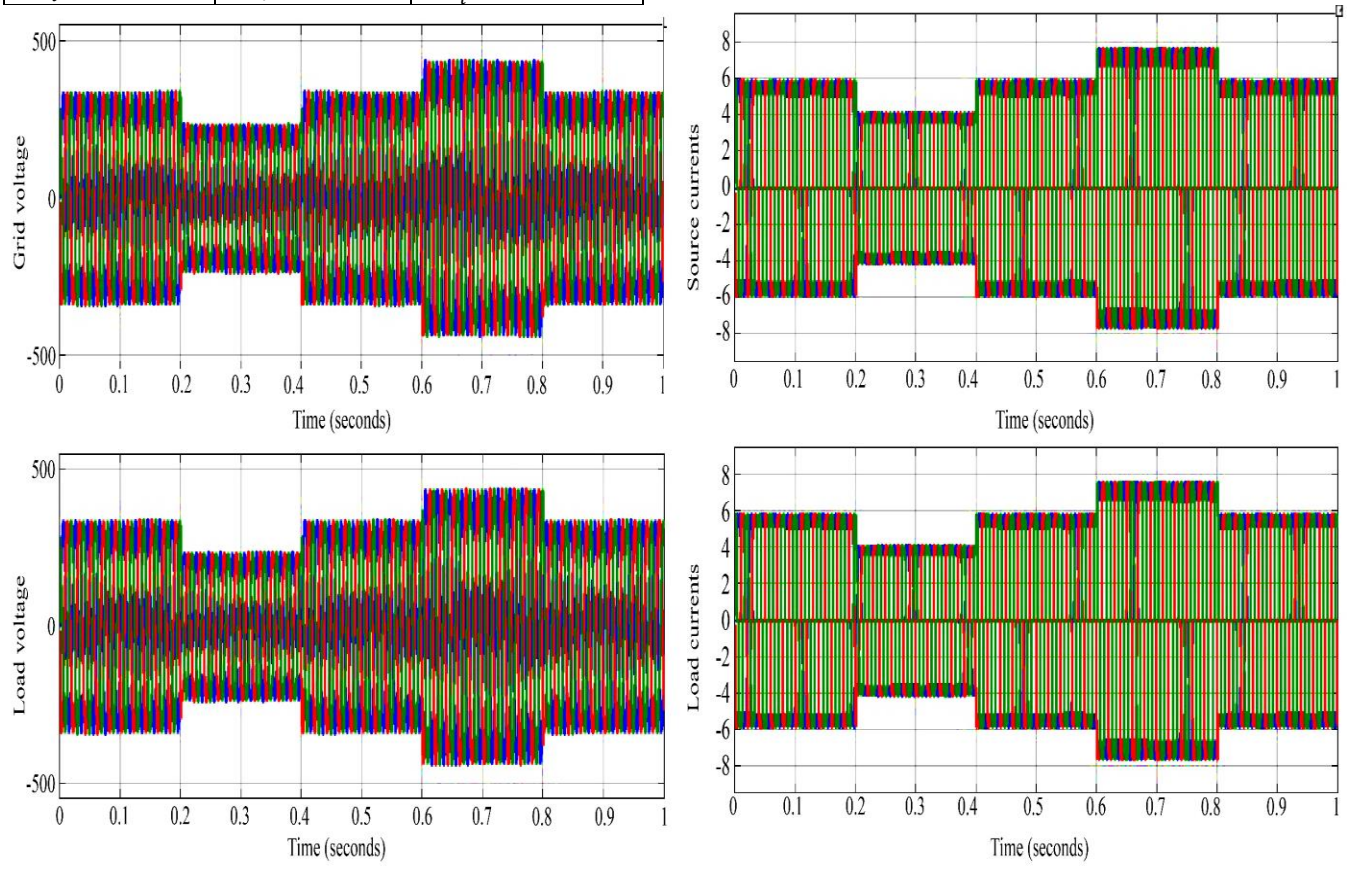

Fig. 8 Source, load voltages and currents without UPQC

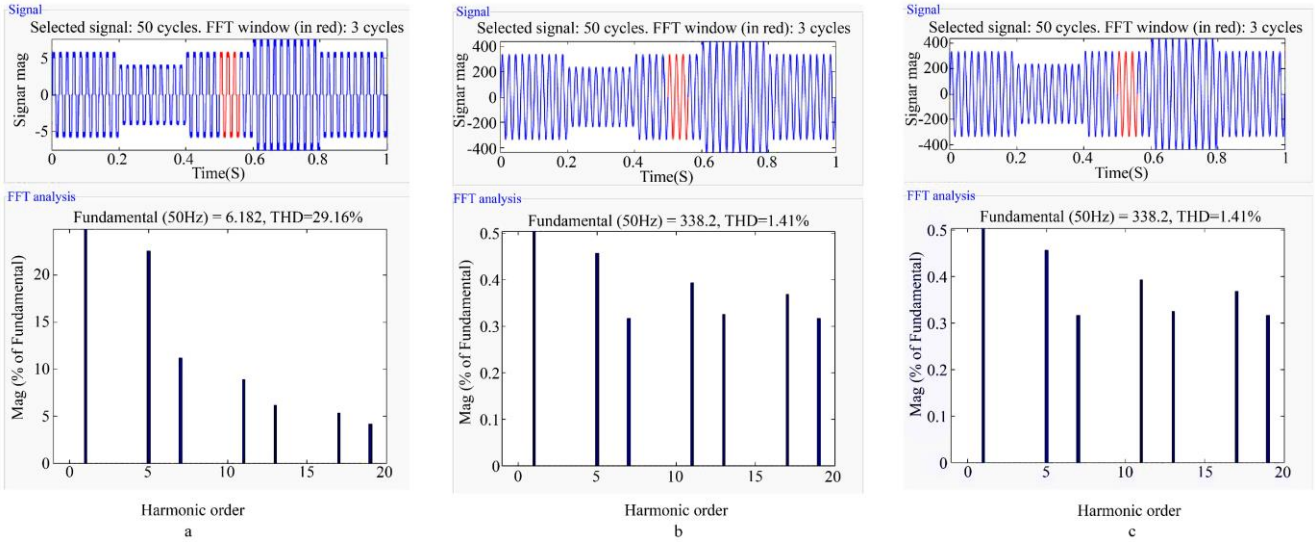

Fig. 9 THD without UPQC a) source current b) source voltage and c) load voltage

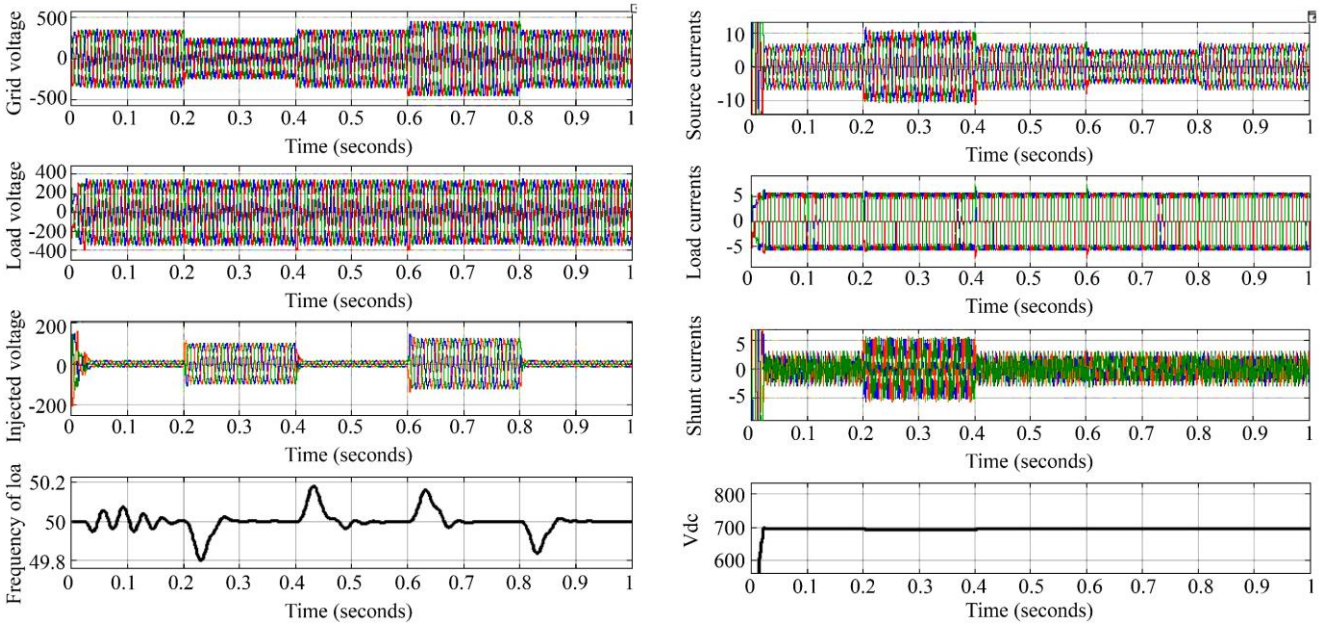

Fig. 10 Voltages and current of source and load with UPQC

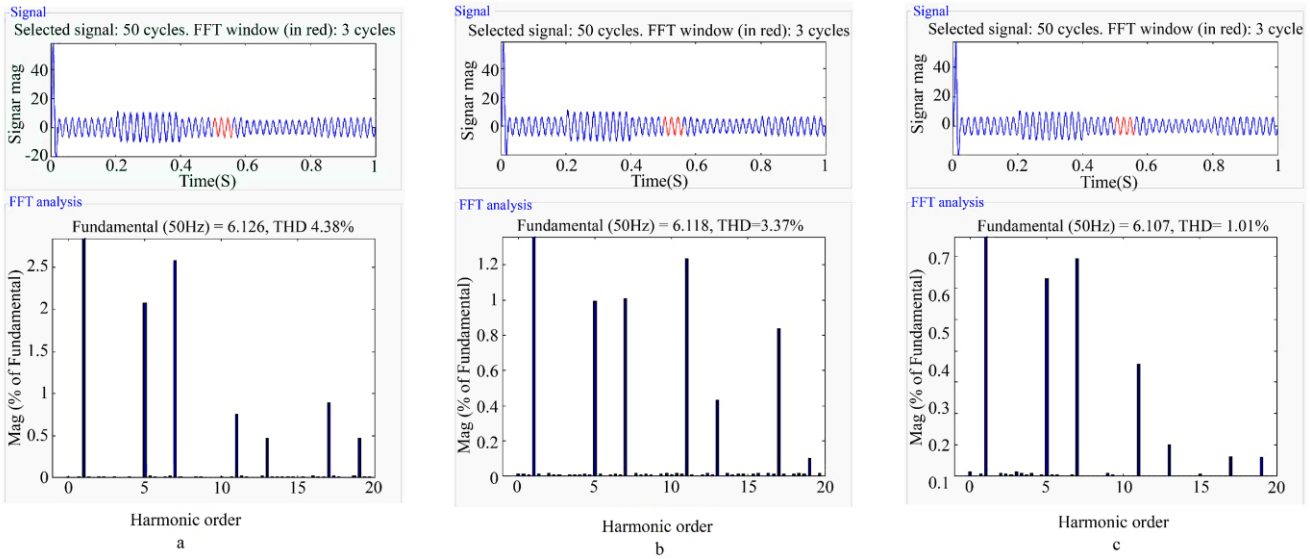

Fig. 11 THDs of source current with a) UPQC-PI b) UPQC-FOPI c) UPQC-SM-FOPI

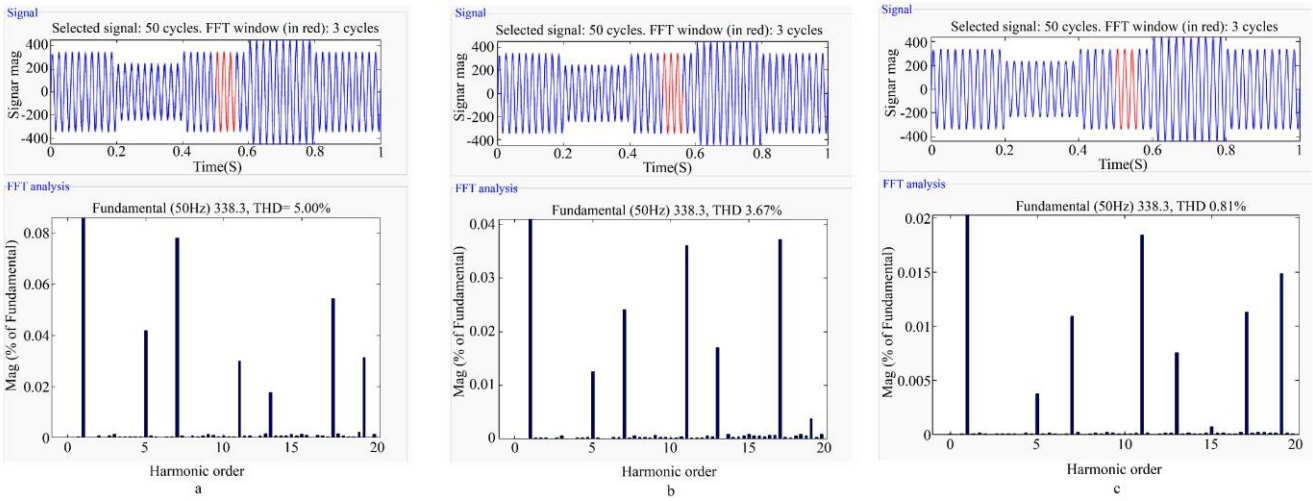

Fig. 12 THDs of Source voltage with a) UPQC-PI b) UPQC-FOPI c) UPQC-SM-FOPI

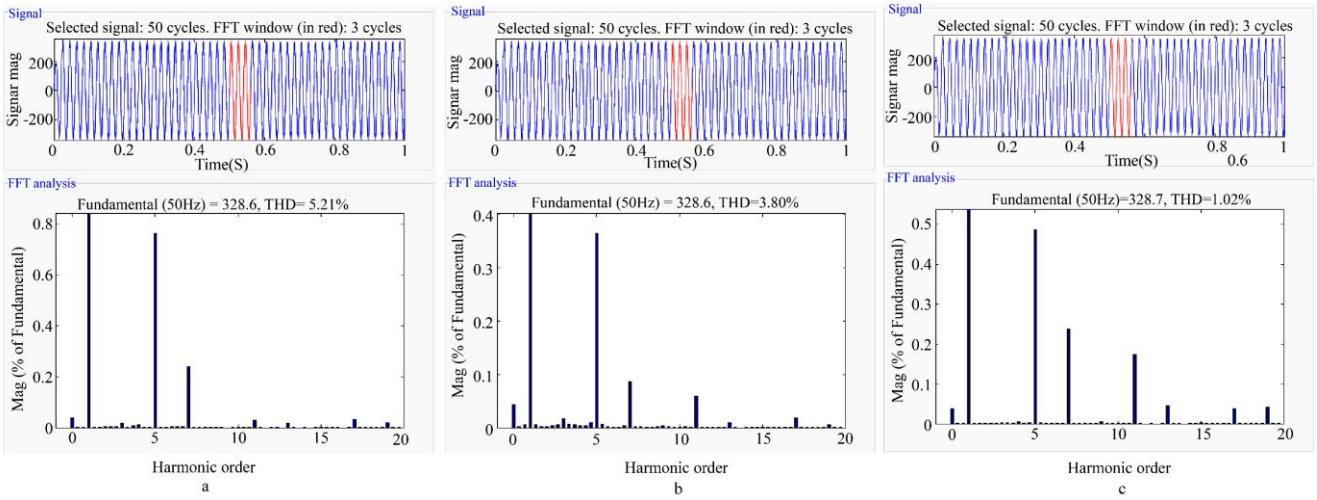

Fig. 13 THDs of Load voltage with a) UPQC-PI, b) UPQC-FOPI, c) UPQC-SM-FOPI

As observed in Figure 8, the sag and swell created in the source (Grid) voltages are introduced on the load side as the UPQC is unavailable. The harmonic content is very high, in the range of 29.16%, as the nonlinear load induces third harmonics into the grid. The THD (Total Harmonic Distortion) is determined using the FFT analysis tool available in the 'powergui' tool of the Simulink library. The system is now updated with UPQC connected with the series converter on the source side and the shunt converter on the load side. As in graphs of Figure 10, the load voltages are compensated by a series converter through series transformers injected as per the difference of the voltage.

The system frequency is maintained at 50Hz with reduced ripple in any given operating condition of voltage sag and swell. The harmonic content in the source current is mitigated by compensation provided by the shunt converter through filter Lf. The DC link voltage is settled at 700V as per the reference given required by the grid system. The DC voltage controller is further updated with FOPI and SM-FOPI, and the simulation is run for the same operating conditions. The THDs of the source current, source voltage and load voltage are taken for each controller and are compared in Figures 11, 12 and 13.

All the THDs are taken at the same time interval of 0.5 sec, and the same number of cycles (three) are considered for the analysis. The SM-FOPI controller gain values vary with respect to error voltage and are shown in Figure 14. As seen in Figure 14, the Kp, Ki and λ values are varied during the time intervals of sag and swell on the system.

With the above FFT analysis tool figures of the THD analysis of voltages and currents, a THD% comparative table 3 is given for validating the best controller for the UPQC. As per Table 3, the THD of the source current is drastically mitigated when the UPQC device is integrated between the source and load. However, the voltages of THDs are increased to the accepted limit for PI and FOPI, but for SM-FOPI controller UPQC, the THDs of all the parameters are reduced to a great extent near 1%.

Table 3. THD comparison

Name of the parameter	No UPQC	PI	FOPI	SM-FOPI
Vsabc	1.41%	5%	3.67%	0.81%
VLabc	1.41%	5.21%	3.8%	1.02%
Isabc	29.16	4.38%	3.37%	1.01%

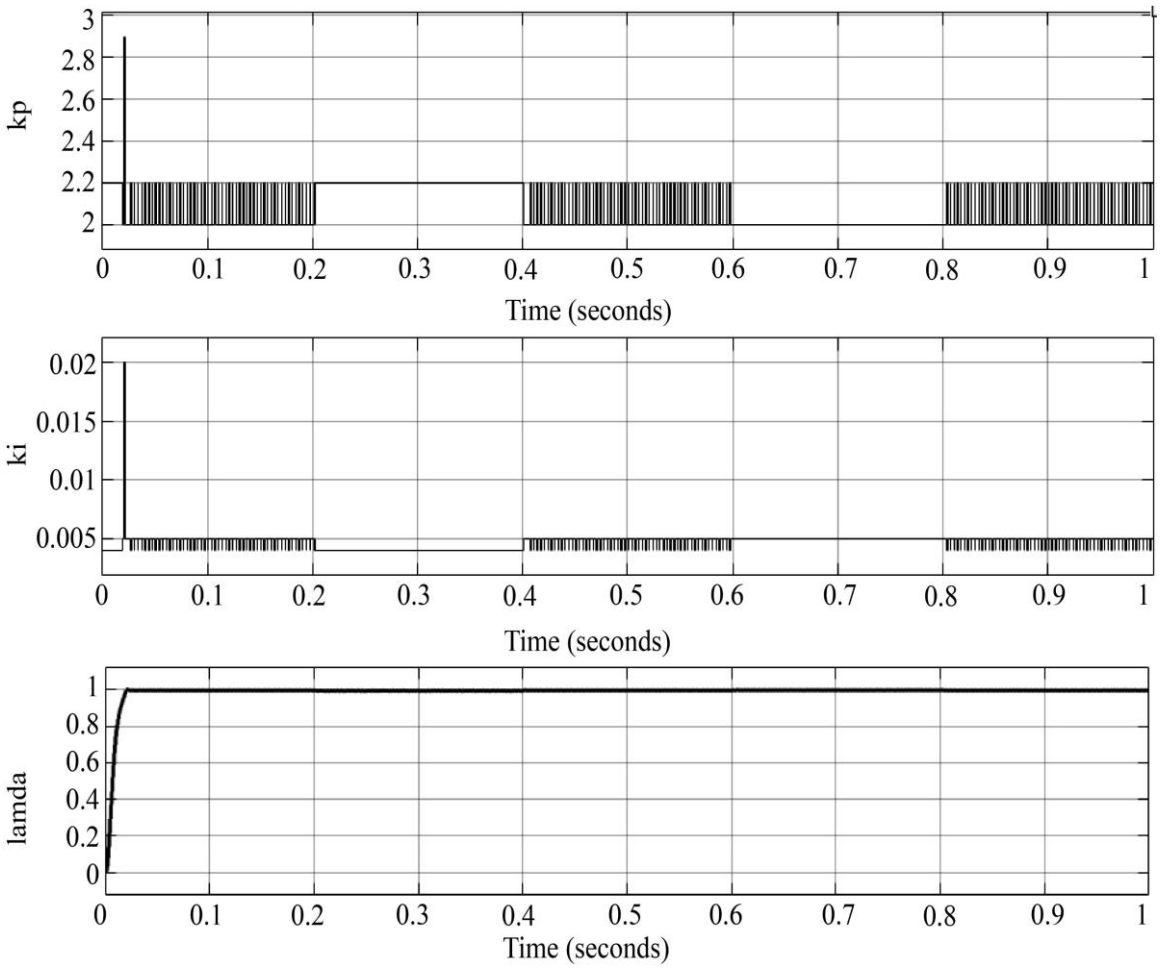

Fig. 14 Kp, Ki and λ gain values in SM-FOPI controller of UPQC

5. Conclusion

As per the given modeling of the test system network, the implementation of the UPQC device with different control modules in the shunt controller is done. The analysis is carried out with mitigation of sag, swell of voltages and harmonics in the currents without and with UPQC device. The design and modeling of adopted control modules in the shunt controller are given in this paper to improve the performance of UPQC. A comparative analysis is carried out on the system with PI, FOPI and SM-FOPI controllers for the determination of the best controller. Harmonic analysis is carried out on the parameters measured with different controllers, validating SM-FOPI as the best control module for the UPQC. The THD of all the voltages and currents is maintained at approximately 1%, making it an ideal choice for operating UPQC in the given operating conditions.

References

[1] Tomasz Tarasiuk et al., "Review of Power Quality Issues in Maritime Microgrids," *IEEE Access*, vol. 9, pp. 81798-81817, 2021. [CrossRef] [Google Scholar] [Publisher Link]

[2] Ammar Ahmed Alkahtani et al., "Power Quality in Microgrids Including Supraharmonics: Issues, Standards, and Mitigations," *IEEE Access*, vol. 8, pp. 127104-127122, 2020. [CrossRef] [Google Scholar] [Publisher Link]

[3] Farzam Nejabatkhah, Yun Wei Li, and Hao Tian, "Power Quality Control of Smart Hybrid AC/DC Microgrids: An Overview," *IEEE Access*, vol. 7, pp. 52295-52318, 2019. [CrossRef] [Google Scholar] [Publisher Link]

[4] Imran Khan, A.S. Vijay, and Suryanarayana Doolla, "Nonlinear Load Harmonic Mitigation Strategies in Microgrids: State of the Art," *IEEE Systems Journal*, vol. 16, no. 3, pp. 4243-4255, 2022. [CrossRef] [Google Scholar] [Publisher Link]

[5] Linghui Meng et al., "Control Strategy of Single-Phase UPQC for Suppressing the Influences of Low-Frequency DC-Link Voltage Ripple," *IEEE Transactions on Power Electronics*, vol. 37, no. 2, pp. 2113-2124, 2022. [CrossRef] [Google Scholar] [Publisher Link]

[6] Rodrigo P. de Lacerda et al., "Six-Leg Single-Phase AC–DC–AC Multilevel Converter with Transformers for UPS and UPQC Applications," *IEEE Transactions on Industry Applications*, vol. 56, no. 5, pp. 5170-5181, 2020. [CrossRef] [Google Scholar] [Publisher Link]

[7] Yahia M. Esmail et al., "Mitigating Power Quality Disturbances in Smart Grid Using FACTS," *Indonesian Journal of Electrical Engineering and Computer Science*, vol. 22, no. 3, pp. 1223-1235, 2021. [CrossRef] [Google Scholar] [Publisher Link]

[8] Sachin Devassy, and Bhim Singh, "Performance Analysis of Solar PV Array and Battery Integrated Unified Power Quality Conditioner for Microgrid Systems," *IEEE Transactions on Industrial Electronics*, vol. 68, no. 5, pp. 4027-4035, 2021. [CrossRef] [Google Scholar] [Publisher Link]

[9] Mythreyee Madhavan, and Nalini Anandan, "Unified Power Quality Control Based Microgrid for Power Quality Enhancement Using Various Controlling Techniques," *Indonesian Journal of Electrical Engineering and Computer Science*, vol. 29, no. 1, pp. 75-84, 2023. [CrossRef] [Google Scholar] [Publisher Link]

[10] Sarita Samal, and Prakash Kumar Hota, "Wind Energy Fed UPQC System for Power Quality Improvement," *Bulletin of Electrical Engineering and Informatics*, vol. 7, no. 3, pp. 495-504, 2018. [CrossRef] [Google Scholar] [Publisher Link]

[11] Alan Santana Felinto et al., "Three-Phase Unified Power Quality Conditioner Based on High-Frequency Link," *IEEE Transactions on Industry Applications*, vol. 58, no. 5, pp. 6397-6407, 2022. [CrossRef] [Google Scholar] [Publisher Link]

[12] Madhusmita Patro, and Kanhu Charan Bhuyan, "Unified Power Quality Conditioner Using Injection Capacitors for Voltage Sag Compensation," *International Journal of Applied Power Engineering*, vol. 6, no. 1, pp. 35-44, 2017. [CrossRef] [Google Scholar] [Publisher Link]

[13] Yeison Alberto Garcés Gómez, Nicolás Toro García, and Fredy EdimerHoyos, "Unit Vector Template Generator Applied to a New Control Algorithm for an UPQC with Instantaneous Power Tensor Formulation, A Simulation Case Study," *International Journal of Electrical and Computer Engineering*, vol. 10, no. 4, pp. 3889-3897, 2020. [CrossRef] [Google Scholar] [Publisher Link]

[14] Amirullah Amirullah, Ontoseno Penangsang, and Adi Soeprijanto, "Matlab/Simulink Simulation of Unified Power Quality Conditioner-Battery Energy Storage System Supplied by PV-Wind Hybrid Using Fuzzy Logic Controller," *International Journal of Electrical and Computer Engineering*, vol. 9, no. 3, pp. 1479-1495, 2019. [CrossRef] [Google Scholar] [Publisher Link]

[15] Preeti Warrier, and Pritesh Shah, "Fractional Order Control of Power Electronic Converters in Industrial Drives and Renewable Energy Systems: A Review," *IEEE Access*, vol. 9, pp. 58982-59009, 2021. [CrossRef] [Google Scholar] [Publisher Link]

[16] Arnau Dòria-Cerezo et al., "Comparison of First- and Second-Order Sliding-Mode Controllers for a DC-DC Dual Active Bridge," *IEEE Access*, vol. 10, pp. 40264-40272, 2022. [CrossRef] [Google Scholar] [Publisher Link]

[17] Ibrahima N. Doye, Khaled Nabil Salama, and Taous-Meriem Laleg-Kirati, "Robust Fractional-Order Proportional-Integral Observer for Synchronization of Chaotic Fractional-Order Systems," *IEEE/CAA Journal of AutomaticaSinica*, vol. 6, no. 1, pp. 268-277, 2019. [CrossRef] [Google Scholar] [Publisher Link]

[18] Aishwarya Apte, Ujjwala Thakar, and Vrunda Joshi, "Disturbance Observer-Based Speed Control of PMSM Using Fractional Order PI Controller," *IEEE/CAA Journal of AutomaticaSinica*, vol. 6, no. 1, pp. 316-326, 2019. [CrossRef] [Google Scholar] [Publisher Link]

[19] S.R. Mudaliyar et al., "Cascaded Fractional Order and Sliding Mode Control for an Autonomous Voltage Source Inverter," *IEEE Power and Energy Society General Meeting*, Portland, OR, USA, pp. 1-5, 2018. [CrossRef] [Google Scholar] [Publisher Link]

[20] Chang Jiang, and Shaohua Zhang, "Power Quality Compensation Strategy of MMC-UPQC Based on Passive Sliding Mode Control," *IEEE Access*, vol. 11, pp. 3662-3679, 2023. [CrossRef] [Google Scholar] [Publisher Link]

[21] Zicheng Li et al., "A Bi-Sliding Mode PI Control of DC-Link Voltage of Three-Phase Three-Wire Shunt Active Power Filter," *IEEE Journal of Emerging and Selected Topics in Power Electronics*, vol. 10, no. 6, pp. 7581-7588, 2022. [CrossRef] [Google Scholar] [Publisher Link]

[22] Ayman Al Zawaideh, and Igor M. Boiko, "Analysis of Stability and Performance of a Cascaded PI Sliding-Mode Control DC–DC Boost Converter via LPRS," *IEEE Transactions on Power Electronics*, vol. 37, no. 9, pp. 10455-10465, 2022. [CrossRef] [Google Scholar] [Publisher Link]